Steady state multiple dark spatial solitons in the biased photorefractive-photovoltaic crystals*

ZHANG Yu-hong (张玉虹)**, **SU Wei** (苏炜), **DUAN Cun-li** (段存丽), **and TIAN Ai-ling** (田爱玲)
College of Optoelectronic Engineering, Xi'an Technological University, Xi'an 710021, China

(Received 26 March 2018; Revised 6 May 2018)
©Tianjin University of Technology and Springer-Verlag GmbH Germany, part of Springer Nature 2018

We theoretically study the evolution of dark solitons in the biased photorefractive-photovoltaic crystal by using beam propagation method (BPM). We find that when the absolute value of the extra bias field is less than the photovoltaic field, the dark screening-photovoltaic (SP) solitons can be observed. The initial width of the dark notch at the entrance face of the crystal is a key parameter for generating an sequence of dark coherent solitons. If the initial width of the dark notch is small, only a fundamental soliton or Y-junction soliton pair is generated. When the initial width of the dark notch is increased, the dark notch tends to split into an odd (or even) number of multiple dark solitons, which realizes a progressive transition from the low-order solitons to a sequence of higher-order solitons.
Document code: A **Article ID:** 1673-1905(2018)05-0367-5
DOI https://doi.org/10.1007/s11801-018-8045-6

Screening-photovoltaic (SP) spatial solitons have been predicted and observed in a photovoltaic-photorefractive (PV-PR) crystal with a biased field. They differ from both the screening solitons and the photovoltaic (PV) solitons in their properties and experimental conditions. The existence of the SP solitons results from both the PV effect and spatially non-uniform screening of the bias field in the biased PV-PR crystal. SP solitons can change into screening solitons when the bulk PV effect is neglected and PV solitons in the closed-circuit case when the external bias field is absent. Thus far, bright[1,2], dark[3,4], and gray[5] SP spatial soliton domains have been predicted in steady state.

In addition, particular interests are the lattice solitons also known as discrete solitons, defect solitons, gap solitons which are supported by the nonlinear periodic systems[6], irrespective of the nature of the nonlinearity or specific structure of the index lattice. So far, defect solitons, gap solitons, discrete solitons in the optically induced photonic lattices[7,8] and in the PT-symmetric optical lattices with nonlocal nonlinearity[9-12] have been investigated in the biased PV-PR crystals. The nonlinear Schrodinger equation that describes the evolution of the light in a periodic array is different from that in the bulk nonlinear PR crystal. The method of solving the nonlinear Schrodinger equation is also different. To find the lattice soliton solution in periodic discrete system, the associated band structure of the optical lattice should be firstly analyzed and then the discrete soliton structure is obtained by using numerical method. The characteristics of lattice solitons are also different from those in the bulk nonlinear PR crystals.

In this paper, we concentrate on the evolution of solitons in the bulk PR nonlinear medium. In 1998, Liu[13] numerically investigated the dynamical evolution of bright SP solitons in biased PV-PR media in the case of neglecting the material loss and the diffusion. In addition, the dynamical evolutions of dark screening solitons[14,15] and dark PV solitons[16-19] have been theoretically and experimentally investigated. However, the dynamical evolution of dark SP spatial solitons in biased PV crystals has not been investigated yet. Thus, we numerically investigate the formation of multiple SP dark solitons in the steady-state regimes by using beam propagation method (BMP). It is worthwhile to note that dark SP solitons evolve from a single dark notch. The initial profile of the dark notch at the entrance of the PV crystal is obtained by solving the nonlinear Schrödinger equation which describes the propagation of the PR spatial soliton. The investigation results show that the splitting of dark SP spatial soliton is possible in biased PP crystals. If the full width half maximum (*FWHM*) of the beam intensity is small, only a fundamental soliton or Y-junction soliton is generated. When the intensity *FWHM* of the input beam is increased, the solitons beam splits into an odd or even number of multiple dark solitons.

For convenience of the analysis, we consider a coherent beam uniform along the y axis that propagates in a biased PV-PR crystal along the z-axis and is allowed to diffract only along the x direction. Meanwhile, we assume that the coherent beam is linearly polarized along the x direction. The PR crystal is assumed to be $LiNbO_3$,

* This work has been supported by the National Natural Science Foundation of China (No.10674176), and the National Foundation of Shaanxi Provincial Department of Education (No.17JK0389).
** E-mail: zhangyh1979@163.com

with its optical *c*-axis oriented along *x* coordinate. Moreover, the external bias electric field and the polarization of the incident optical beam are also parallel to the *c*-axis. Under these conditions, the perturbed refractive index along the *x*-axis is given by $(n'_e)^2 = n_e^2 - n_e^4 r_{33} E_{sc}$, where n_e is the unperturbed extraordinary index of refraction, r_{33} is the electro-optic coefficient of the PR crystal, and E_{sc} is the induced space-charge electric field. Therefore, the refractive index variation that is due to space-charge field E_{sc} is $\Delta n_e = -0.5 n_e^3 r_{33} E_{sc}$. Based on the band-transport model, the equation for the 1D PR space charge field E_{sc}[1] by neglecting the material loss and the diffusion in a biased PV-PR crystal is given by

$$E_{sc} = E_0 \frac{I_\infty + I_d}{I + I_d} + E_p \frac{I_\infty + I_d}{I + I_d} \quad , \tag{1}$$

where $E_p=\kappa\gamma N_A/e\mu$ is the PV field constant, and E_0 is the value of the space-charge field in the dark regions of the crystal. If the spatial extent of the optical wave is much less than the *x*-width *L* of the PR crystal, under a constant voltage bias *V*, E_0 is approximately given by V/L. Strictly speaking, under strong dynamical evolution conditions, E_0 is not a constant but instead may vary with respect to *z*. However, if the *x*-width *W* of the crystal is considerably bigger than the spatial extent of the optical beam, E_0 will become relatively insensitive to the wave's dynamics and hence can be treated as a constant[20]. By integrating numerically the nonlinear propagation equation, it is found that the soliton beam evolution is approximately adiabatic.

Theoretically, the solution for a one-dimensional SP dark soliton propagating along the *z*-axis is described by the nonlinear Schrödinger equation as:

$$\mathrm{i}\phi_z + \frac{1}{2k}\phi_{xx} - \frac{k_0}{2}(n_e^3 r_{33} E_{sc})\phi = 0 \ , \tag{2}$$

where $\phi(x, z)$ is the slowly varying amplitude of the input optical field, λ_0 is the free-space wavelength of the light wave, $k_0=2\pi/\lambda_0$ and $k=k_0 n_e$ are the wave numbers in the free-space and PV-PR crystal, respectively.

Let us adopt the following dimensionless coordinates and variables: $\xi=z/kx_0^2$, $s=x/x_0$, $\phi=(2\eta I_d/n_e)^{1/2}U$, where x_0 is an arbitrary spatial width and the beam power density has been scaled with respect to the dark irradiance I_d. The normalized envelope *U* obeys the following dynamical evolution equation:

$$\mathrm{i}U_\xi + \frac{1}{2}U_{ss} - \beta\frac{1+\rho}{1+|U|^2}U - \alpha\frac{\rho-|U|^2}{1+|U|^2}U = 0 \ , \tag{3}$$

where $\rho=I_{max}/I_d$, $\beta=1/2(k_0x_0)^2 n_e^4 r_{33} E_0$, $\alpha=1/2(k_0x_0)^2 n_e^4 r_{33} E_p$. The values of α and β depend on PV field E_p and the external biased field E_0, respectively. The sign of β depends on the polarity of E_0. However, the sign of α depends on the characteristic of the crystal and the polarization of the optical beam. Since all observations indicate a negative perturbation in the index for $LiNbO_3$ crystal, α is negative.

The solution of a fundamental dark soliton can be written as $U(s,\xi)=\rho^{1/2}y(s)\exp(\mathrm{i}\upsilon\xi)$, where υ is a nonlinear shift of the propagation constant and $y(s)$ is a normalized odd function. Substituting this form of $U(s,\xi)$ into Eq.(3) yields

$$y'' - 2\upsilon y - 2\beta\frac{1+\rho}{1+\rho|y|^2}y - 2\alpha\rho\frac{1-|y|^2}{1+\rho|y|^2}y = 0 \ . \tag{4}$$

Furthermore, by applying boundary conditions of dark solitons $y'(\infty)=y''(\infty)=0$ and $y(s\to\pm\infty)=\pm1$ in Eq.(4), the soliton propagation constant can be obtained as $\upsilon=-\beta$. In our calculation, we numerically integrate Eq.(4) and apply boundary conditions of dark soliton to obtain

$$y'^2 = -2(\alpha+\beta)\left[(y^2-1) - \frac{\rho+1}{\rho}\ln\left(\frac{1+\rho y^2}{1+\rho}\right)\right] \ . \tag{5}$$

It can be readily shown that the quantity in brackets in Eq.(5) remains positive for all values of $y^2\le1$, and thus $(\beta+\alpha)$ must be negative so that $y'^2>0$. When $\alpha<0$ (for example, $LiNbO_3$), if $|\alpha|>|\beta|$, dark SP solitons can be observed whether the polarity (the sign of β) of the external bias is positive or negtive[1]. Thus the formation of the SP spatial solitons depends not only on the external bias field but also on the photovoltaic term. In our simulations, the crystal-dependent parameters of the biased PV-PR crystal are those of the $LiNbO_3$ crystal extracted from the same boule[3], i.e., the unperturbed refractive index $n_e=2.2$, the PV field $E_p=4\times10^6$ V/m, the electro-optical coefficient $r_{33}=30\times10^{-12}$ m/V, the transverse distance of the crystal $l=1$ cm, and the free-space wavelength of the laser beam $\lambda=0.5$ μm. Thus, dark SP solitons can be obtained, provided the extra bias voltage is less than 40 kV. Eq.(4) can be integrated numerically by a fourth Runge-Kutta algorithm combined with initial conditions $y'(0)$ and $y(0)$ to yield the spatial profile of the fundamental SP dark soliton. Fig.1 shows the normalized steady-state SP dark soliton intensity profile. From Fig.1, we note that when the extra bias field ($E_0=V/l$) is less than the PV field E_p, the value of the extra bias voltage will affect the *FWHM* of the dark SP spatial solitons.

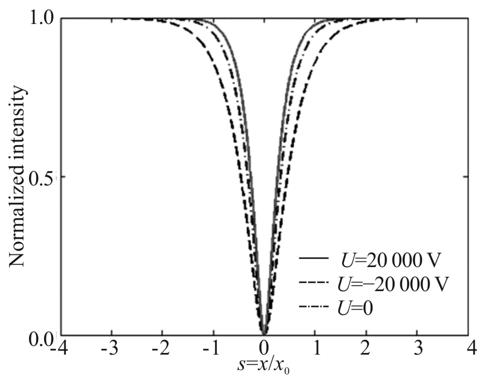

Fig.1 Normalized intensity profiles of dark SP spatial solitons for ρ=5

From Fig.2, we note that the existence curve of the fundamental SP dark soliton gives the relationship among the solitons' amplitude, width and nonlinearity in the medium. The *FWHM* of the fundamental soliton intensity is a function of the ratio (ρ) of soliton peak intensity I_{max} to dark irradiance I_d. When ρ is small, the dark solitons' intensity *FWHM* decreases monotonously and acutely with ρ. Then, the width of SP solitons is nearly invariable.

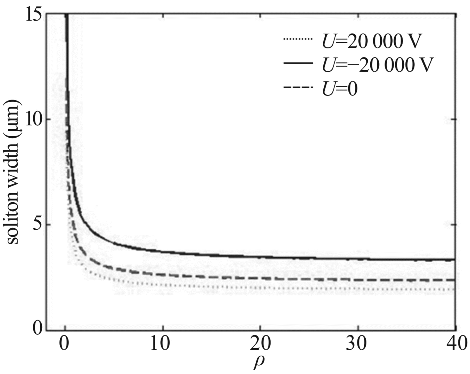

Fig.2 The dark SP solitons *FWHM* as a function of *ρ*

Dark spatial solitons can be generated by launching an optical beam with two different initial conditions into a self-defocusing PR (or Kerr) nonlinear medium. One is the odd initial condition, which provides a π phase jump in the center of a beam while keeping the amplitude uniform across the beam. The other is the even initial condition, which provides an amplitude depression at the center and an even symmetry in the phase of the beam. In this paper, we simulate numerically the evolution of the dark notch generated by the two initial conditions inside the crystal in the steady state regime.

In the following simulations, we change the input width of the dark notch Δx to achieve the transformation from a fundamental soliton or a Y-junction soliton to the multiple solitons. Firstly, we calculate $\varphi(s, 0)$ by solving Eq.(4) numerically with a fourth Runge-Kutta method and then expand the soliton's intensity *FWHM*. Then, Eq.(3) is solved numerically by BPM to obtain the evolution process of the multiple solitons inside the PR crystal. In our calculation, we divide the propagation distance into many steps in which the step size $d\xi$ is designated as 0.03, i.e., dz=1 μm. In every step, the diffraction effect is first considered exclusively, and then only the nonlinear term is calculated. The step size used is 10^{-3} and the calculated relative error and absolute error in the simulation process are 10^{-6}.

For an odd-phased input beam, when the ratio of soliton peak intensity to dark irradiance is ρ=5, a solution of Eq.(4) can be found and it describes a fundamental dark soliton with *FWHM*=4.1 μm. For illustrating this point, the evolution process of the soliton profile is plotted in Fig.3(a) with a 1 cm propagation distance. A constant beam profile is obtained throughout the crystal. When we enlarge the dark notch, a pair of less visible dark notches appears symmetrically on both sides of the central dark notch. For instance, Fig.3(b) shows that the triple-solitons structure consists of two side lobes and a central lobe when the initial width of the input dark notch is 15 μm. The minimum intensity of the two side lobes is less visible. If the width of initial input dark notch is further increased, a secondary set of lobes with less visibility symmetrically starts to appear on the two sides of the triple-soliton structure. Fig.3(c) shows the N=5 splitting found for Δx_5=23 μm. If we further increase intensity *FWHM* of dark notch, we can observe N=7 solitons splitting for Δx_7=36 μm. Therefore, the odd-phased beam tends to split into the odd-number sequence of multiple dark solitons.

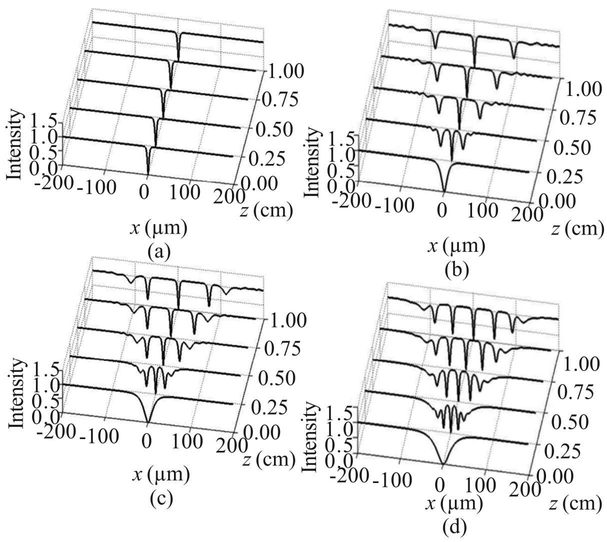

Fig.3 Formation of the multiple dark SP solitons under odd initial conditions (*ρ*=5, *z*=1 cm, *U*=-20 000 V): (a) Propagation of a 4.1-μm-wide fundamental dark soliton; (b) A 15-μm-wide dark notch splitting into three dark soliton stripes; (c) A 23-μm-wide dark notch splitting into five dark soliton stripes; (d) A 36-μm-wide dark notch splitting into seven dark soliton stripes

For an even-phased input beam, the dark notch always tends to split into two when the intensity *FWHM* of initial dark notch is small. Fig.4(a) shows the Y splitting found for Δx_2=10 μm. The width of each lobe and the deep of the intensity are equal. As the intensity *FWHM* of the dark notch is further increased, in a manner similar to that of an odd-phased beam, more secondary sets of lobes appear symmetrically on two sides of the Y-junction soliton splitting. Fig.4(b) shows the N=4 splitting found for Δx_4=18 μm. Fig.4(c) shows the N=6 soliton splitting for Δx_6=30 μm. If we further increase the width of the dark notch, more soliton pairs with less visibility will appear in two sides, forming the higher-order even-number sequence of multiple dark SP spatial solitons.

From Fig.3 and Fig.4, we note that the generation of multiple dark SP solitons depends on the initial input width of the dark notch for a fixed input optical intensity. The number of solitons increases with the width of the initial dark notch. When multiple solitons are generated, the separations between adjacent dark solitons become smaller. In addition, soliton pairs become progressively less visible as their transverse distance from the central dark soliton increases. The results reveal the similar property of the multiple dark screening solitons[14,15] and photovoltaic solitons[16-19].

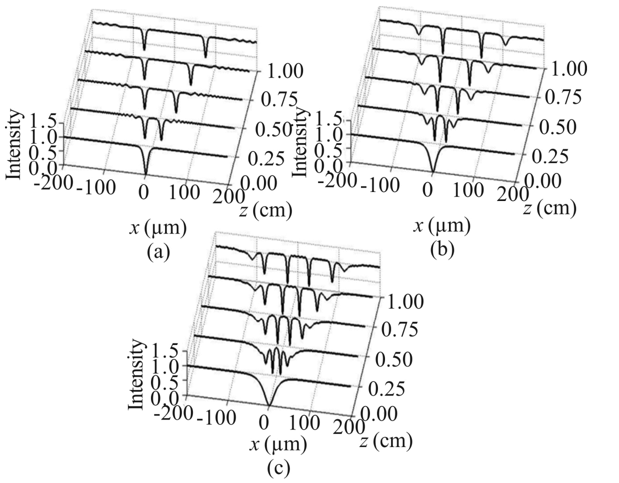

Fig.4 Formation of the multiple dark SP solitons under even initial conditions (*ρ*=5, *z*=1 cm, *U*=-20 000 V): (a) Propagation of a 10-μm-wide Y-junction dark solitons pair; (b) A 18-μm-wide dark notch splitting into four dark soliton stripes; (c) A 30-μm-wide dark notch splitting into six dark soliton stripes

In addition, according to theory of SP solitons[1,3], SP solitons are as a unity form of screening solitons and PV solitons in short and open circuit realization. Screening solitons and PV solitons in short and open circuits can be derived from these solitons. When the bulk PV effect is neglected, SP solitons can change into screening solitons. Accordingly, α=0 in Eqs.(3)—(5), the evolution result of solitons is shown in Fig.5(a). When the external biased field is absent, the SP solitons change into PV solitons in open circuit condition. Accordingly, β=0 in Eqs.(3)—(5), the evolution result of solitons is shown in Fig.5(b). From Fig.5, we note that the evolution results of these three types of solitons are similar. The only difference is that the magnitude of the nonlinearity is different, so the number of multiple dark soltions is different. Thus, multiple dark SP solitons have similar property to the multiple dark screening solitons and PV solitons.

In this section, we discuss the influence of the biased voltage on the evolution of the dark SP spatial solitons. From Fig.6, we find that the value of the biased voltage is negative, the number of solitons splitting is less, and solitons splitting needs larger nonlinearity. The larger the bias is, the larger the nonlinearity required to form the multiple dark solitons when the width of the input dark notch is fixed.

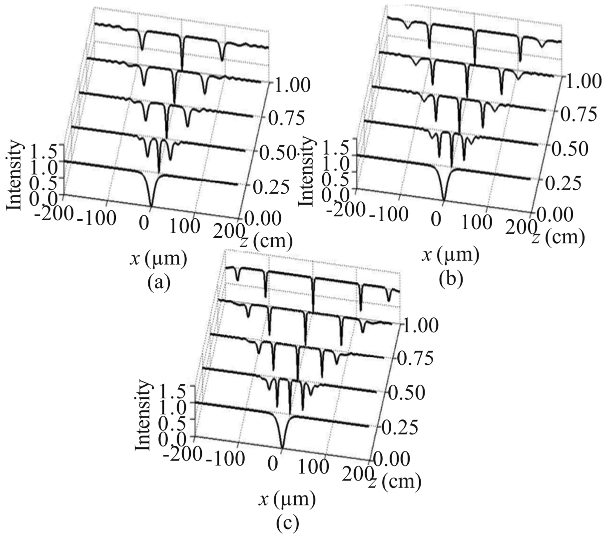

Fig.5 The dynamical evolution of solitons when the width of the input dark notch is 15 μm: (a) PV field is neglected; (b) Extra biased voltage is absent; (c) PV field and extra biased voltage are both existent.

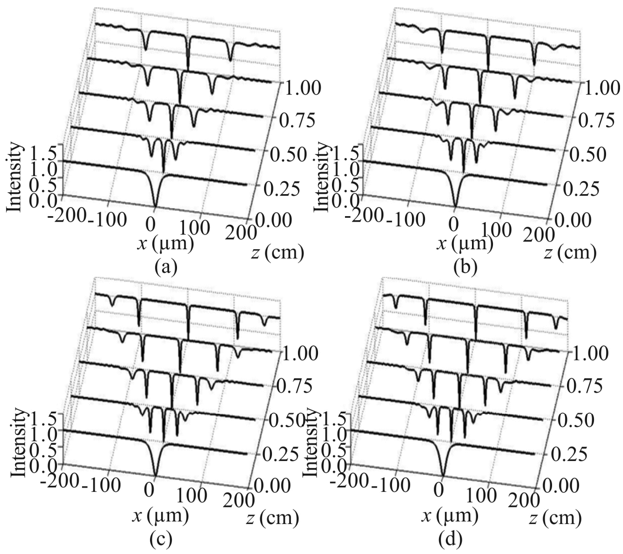

Fig.6 The influence of the bias field on the number of multiple dark SP spatial solitons (The width of input dark notch is 15 μm): (a) *U*=-20 000 V; (b) *U*=-10 000 V; (c) *U*=10 000 V, (d) *U*=20 000 V

In conclusion, we simulate the evolution of the dark solitons in a biased PV-PR crystal by using BPM. The results indicate that the steady state multiple dark SP spatial solitons sequence can be formed by expanding the width of the dark notch that was launched on the front surface of the biased PV-PR crystals. The multiple dark SP spatial solitons sequence has the similar property to the multiple dark screening solitons and photovoltaic solitons. The more the solitons, the wider the dark notch. The lower the visibility, the wider the solitons, and the farther the soliton pairs are from the center.

References

[1] S. Konar and Biswas Anjan, Optical Materials **35**, 2581 (2013).

[2] A. Keshavarz and M. Kamranfard, Optik **122**, 235 (2011).

[3] Katti Aavishkar and Yadav R.A, Physical Letters A **381**, 166 (2017).

[4] Konar S, Shekhar Shashank and Hong Woo-Pyo, Optics and Laser Technology **42**, 1294 (2010).

[5] Ji Xuan-meng, Jiang Qi-chang and Liu Jin-song, Optik **122**, 1848 (2011).

[6] Huang JG, Christian JM and McDonald GS, Journal of Nonlinear Optics Physics & Materials **26**, 1750009 (2017).

[7] Lu ke-qing, Guo Jian-bang, Li Ke-hao, Chen wei-jun, Sun Tong-tong, Yao Feng-xue, Niu Ping-juan and Xu Jing-jun, Optical Materials **34**, 1277 (2012).

[8] Hui Juan-li, Lu Ke-qing, Zhang Bao-ju, Zhang Jun and Xing Hai-ying, Optics Laser Technology **75**, 57 (2015).

[9] Hong Woo-Pyo and Jung Young-Dae, Physics Letters A **379**, 676 (2015).

[10] Li Zhi, Shi Shuang, Ren Xiao-ping and Wang Hong, Journal of Nonlinear Optics Physics & Materials **24**, 1550024 (2015).

[11] Hu Su-mei, Ma Xue-kai, Lu Da-quan, Zheng Yi-zhou and Hu Wei, Physical Review A **85**, 043826 (2012).

[12] Hu Su-mei, Lu Da-quan, Ma Xue-kai, Guo Qi and Hu Wei, European Physics Letters **98**, 14006 (2012).

[13] Liu Jin-song, Chinese Journal of Laser B **10**, 347 (2001).

[14] Chen Zhi-gang, Mordechai Segev and Demetrios N Christodoulides, Reports on Progress in Physics **75**, 086401 (2012).

[15] Zhao Mi-Zhou, Zhang Guang-yong, Chen Guo-zhen and Zhang Xiao-qing, Optik **127**, 10084 (2016).

[16] Zhang Yu-hong, Lu Ke-qing, Guo Jian-bang and Long Xue-wen, Pramana-Journal of Physics **78**, 265 (2012).

[17] Zhang Mei-zhi, Huo Guang-wen, Duan Zuo-liang, Hui Zhan-qiang and Zeng Xiang-mei, Journal of Nonlinear Optical Physics & Materials **22**, 1350032 (2013).

[18] Zhang Yu-hong, Lu Ke-qing Guo Jian-bao, Li Ke-hao and Liu Bao-yuan, European Physical Journal D **66**, 65 (2012).

[19] Zhang Yu-hong, Hu Xiao-hong, Lu Ke-qing, Liu Bao-yuan, Liu Wang-yun and Guo Rong-li, Journal of Optical Technology **80**, 135 (2013).

[20] Demetrios N Christodoulides and M. I. Carvalho, Journal of the Optical Society of America B-Optical Physics **12**, 1628 (1995).